EUROPEAN ORGANIZATION FOR NUCLEAR RESEARCH (CERN)

CERN-EP/2003-077
November 26, 2003

Absolute mass lower limit for the lightest neutralino of the MSSM from e^+e^- data at $\sqrt{s}$ up to 209 GeV

The ALEPH Collaboration*)

Abstract

Charginos and neutralinos are searched for in the data collected by the ALEPH experiment at LEP for centre-of-mass energies up to 209 GeV. The negative result of these searches is combined with those from searches for sleptons and Higgs bosons to derive an absolute lower limit of 43.1 $\mathrm{GeV/c^2}$ on the mass of the lightest supersymmetric particle (LSP), assumed to be the lightest neutralino. This limit is obtained in the framework of the MSSM with R-parity conservation and with gaugino and sfermion mass unification at the GUT scale and assuming no mixing in the stau sector. The LSP limit degrades only slightly to 42.4 $\mathrm{GeV/c^2}$ if stau mixing is considered. Within the more constrained framework of minimal supergravity, the limit is 50 $\mathrm{GeV/c^2}$.

Submitted to Physics Letters B

*) See next pages for the list of authors

The ALEPH Collaboration

A. Heister, S. Schael

Physikalisches Institut das RWTH-Aachen, D-52056 Aachen, Germany

R. Barate, R. Brunelière, I. De Bonis, D. Decamp, C. Goy, S. Jézéquel, J.-P. Lees, F. Martin, E. Merle, M.-N. Minard, B. Pietrzyk, B. Trocmé

Laboratoire de Physique des Particules (LAPP), IN^{2}P^3-CNRS, F-74019 Annecy-le-Vieux Cedex, France

S. Bravo, M.P. Casado, M. Chmeissani, J.M. Crespo, E. Fernandez, M. Fernandez-Bosman, Ll. Garrido,[15] M. Martinez, A. Pacheco, H. Ruiz

Institut de Física d'Altes Energies, Universitat Autònoma de Barcelona, E-08193 Bellaterra (Barcelona), Spain[7]

A. Colaleo, D. Creanza, N. De Filippis, M. de Palma, G. Iaselli, G. Maggi, M. Maggi, S. Nuzzo, A. Ranieri, G. Raso,[24] F. Ruggieri, G. Selvaggi, L. Silvestris, P. Tempesta, A. Tricomi,[3] G. Zito

Dipartimento di Fisica, INFN Sezione di Bari, I-70126 Bari, Italy

X. Huang, J. Lin, Q. Ouyang, T. Wang, Y. Xie, R. Xu, S. Xue, J. Zhang, L. Zhang, W. Zhao

Institute of High Energy Physics, Academia Sinica, Beijing, The People's Republic of China[8]

D. Abbaneo, T. Barklow,[26] O. Buchmüller,[26] M. Cattaneo, B. Clerbaux,[23] H. Drevermann, R.W. Forty, M. Frank, F. Gianotti, J.B. Hansen, J. Harvey, D.E. Hutchcroft,[30], P. Janot, B. Jost, M. Kado,[2] P. Mato, A. Moutoussi, F. Ranjard, L. Rolandi, D. Schlatter, G. Sguazzoni, F. Teubert, A. Valassi, I. Videau

European Laboratory for Particle Physics (CERN), CH-1211 Geneva 23, Switzerland

F. Badaud, S. Dessagne, A. Falvard,[20] D. Fayolle, P. Gay, J. Jousset, B. Michel, S. Monteil, D. Pallin, J.M. Pascolo, P. Perret

Laboratoire de Physique Corpusculaire, Université Blaise Pascal, IN^{2}P^3-CNRS, Clermont-Ferrand, F-63177 Aubière, France

J.D. Hansen, J.R. Hansen, P.H. Hansen, A.C. Kraan, B.S. Nilsson

Niels Bohr Institute, 2100 Copenhagen, DK-Denmark[9]

A. Kyriakis, C. Markou, E. Simopoulou, A. Vayaki, K. Zachariadou

Nuclear Research Center Demokritos (NRCD), GR-15310 Attiki, Greece

A. Blondel,[12] J.-C. Brient, F. Machefert, A. Rougé, H. Videau

Laoratoire Leprince-Ringuet, Ecole Polytechnique, IN^{2}P^3-CNRS, F-91128 Palaiseau Cedex, France

V. Ciulli, E. Focardi, G. Parrini

Dipartimento di Fisica, Università di Firenze, INFN Sezione di Firenze, I-50125 Firenze, Italy

A. Antonelli, M. Antonelli, G. Bencivenni, F. Bossi, G. Capon, F. Cerutti, V. Chiarella, P. Laurelli, G. Mannocchi,[5] G.P. Murtas, L. Passalacqua

Laboratori Nazionali dell'INFN (LNF-INFN), I-00044 Frascati, Italy

J. Kennedy, J.G. Lynch, P. Negus, V. O'Shea, A.S. Thompson

Department of Physics and Astronomy, University of Glasgow, Glasgow G12 8QQ,United Kingdom[10]

S. Wasserbaech

Utah Valley State College, Orem, UT 84058, U.S.A.

R. Cavanaugh,[4] S. Dhamotharan,[21] C. Geweniger, P. Hanke, V. Hepp, E.E. Kluge, A. Putzer, H. Stenzel,

K. Tittel, M. Wunsch[19]

Kirchhoff-Institut für Physik, Universität Heidelberg, D-69120 Heidelberg, Germany[16]

R. Beuselinck, W. Cameron, G. Davies, P.J. Dornan, M. Girone,[1] R.D. Hill, N. Marinelli, J. Nowell, S.A. Rutherford, J.K. Sedgbeer, J.C. Thompson,[14] R. White

Department of Physics, Imperial College, London SW7 2BZ, United Kingdom[10]

V.M. Ghete, P. Girtler, E. Kneringer, D. Kuhn, G. Rudolph

Institut für Experimentalphysik, Universität Innsbruck, A-6020 Innsbruck, Austria[18]

E. Bouhova-Thacker, C.K. Bowdery, D.P. Clarke, G. Ellis, A.J. Finch, F. Foster, G. Hughes, R.W.L. Jones, M.R. Pearson, N.A. Robertson, M. Smizanska

Department of Physics, University of Lancaster, Lancaster LA1 4YB, United Kingdom[10]

O. van der Aa, C. Delaere,[28] G.Leibenguth,[31] V. Lemaitre[29]

Institut de Physique Nucléaire, Département de Physique, Université Catholique de Louvain, 1348 Louvain-la-Neuve, Belgium

U. Blumenschein, F. Hölldorfer, K. Jakobs, F. Kayser, K. Kleinknecht, A.-S. Müller, B. Renk, H.-G. Sander, S. Schmeling, H. Wachsmuth, C. Zeitnitz, T. Ziegler

Institut für Physik, Universität Mainz, D-55099 Mainz, Germany[16]

A. Bonissent, P. Coyle, C. Curtil, A. Ealet, D. Fouchez, P. Payre, A. Tilquin

Centre de Physique des Particules de Marseille, Univ Méditerranée, IN^{2}P^3-CNRS, F-13288 Marseille, France

F. Ragusa

Dipartimento di Fisica, Università di Milano e INFN Sezione di Milano, I-20133 Milano, Italy.

A. David, H. Dietl,[32] G. Ganis,[27] K. Hüttmann, G. Lütjens, W. Männer[32], H.-G. Moser, R. Settles, M. Villegas, G. Wolf

Max-Planck-Institut für Physik, Werner-Heisenberg-Institut, D-80805 München, Germany[16]

J. Boucrot, O. Callot, M. Davier, L. Duflot, J.-F. Grivaz, Ph. Heusse, A. Jacholkowska,[6] L. Serin, J.-J. Veillet, J.-B. de Vivie de Régie[33]

Laboratoire de l'Accélérateur Linéaire, Université de Paris-Sud, IN^{2}P^3-CNRS, F-91898 Orsay Cedex, France

P. Azzurri, G. Bagliesi, T. Boccali, L. Foà, A. Giammanco, A. Giassi, F. Ligabue, A. Messineo, F. Palla, G. Sanguinetti, A. Sciabà, P. Spagnolo, R. Tenchini, A. Venturi, P.G. Verdini

Dipartimento di Fisica dell'Università, INFN Sezione di Pisa, e Scuola Normale Superiore, I-56010 Pisa, Italy

O. Awunor, G.A. Blair, G. Cowan, A. Garcia-Bellido, M.G. Green, T. Medcalf, A. Misiejuk, J.A. Strong, P. Teixeira-Dias

Department of Physics, Royal Holloway & Bedford New College, University of London, Egham, Surrey TW20 OEX, United Kingdom[10]

R.W. Clifft, T.R. Edgecock, P.R. Norton, I.R. Tomalin, J.J. Ward

Particle Physics Dept., Rutherford Appleton Laboratory, Chilton, Didcot, Oxon OX11 OQX, United Kingdom[10]

B. Bloch-Devaux, D. Boumediene, P. Colas, B. Fabbro, E. Lançon, M.-C. Lemaire, E. Locci, P. Perez, J. Rander, B. Tuchming, B. Vallage

CEA, DAPNIA/Service de Physique des Particules, CE-Saclay, F-91191 Gif-sur-Yvette Cedex, France[17]

A.M. Litke, G. Taylor

Institute for Particle Physics, University of California at Santa Cruz, Santa Cruz, CA 95064, USA[22]

C.N. Booth, S. Cartwright, F. Combley,[25] P.N. Hodgson, M. Lehto, L.F. Thompson

Department of Physics, University of Sheffield, Sheffield S3 7RH, United Kingdom[10]

A. Böhrer, S. Brandt, C. Grupen, J. Hess, A. Ngac, G. Prange

Fachbereich Physik, Universität Siegen, D-57068 Siegen, Germany[16]

C. Borean, G. Giannini

Dipartimento di Fisica, Università di Trieste e INFN Sezione di Trieste, I-34127 Trieste, Italy

H. He, J. Putz, J. Rothberg

Experimental Elementary Particle Physics, University of Washington, Seattle, WA 98195 U.S.A.

S.R. Armstrong, K. Berkelman, K. Cranmer, D.P.S. Ferguson, Y. Gao,[13] S. González, O.J. Hayes, H. Hu, S. Jin, J. Kile, P.A. McNamara III, J. Nielsen, Y.B. Pan, J.H. von Wimmersperg-Toeller, W. Wiedenmann, J. Wu, Sau Lan Wu, X. Wu, G. Zobernig

Department of Physics, University of Wisconsin, Madison, WI 53706, USA[11]

G. Dissertori

Institute for Particle Physics, ETH Hönggerberg, 8093 Zürich, Switzerland.

---

[1]Also at CERN, 1211 Geneva 23, Switzerland.

[2]Now at Fermilab, PO Box 500, MS 352, Batavia, IL 60510, USA

[3]Also at Dipartimento di Fisica di Catania and INFN Sezione di Catania, 95129 Catania, Italy.

[4]Now at University of Florida, Department of Physics, Gainesville, Florida 32611-8440, USA

[5]Also Istituto di Cosmo-Geofisica del C.N.R., Torino, Italy.

[6]Also at Groupe d'Astroparticules de Montpellier, Université de Montpellier II, 34095, Montpellier, France.

[7]Supported by CICYT, Spain.

[8]Supported by the National Science Foundation of China.

[9]Supported by the Danish Natural Science Research Council.

[10]Supported by the UK Particle Physics and Astronomy Research Council.

[11]Supported by the US Department of Energy, grant DE-FG0295-ER40896.

[12]Now at Departement de Physique Corpusculaire, Université de Genève, 1211 Genève 4, Switzerland.

[13]Also at Department of Physics, Tsinghua University, Beijing, The People's Republic of China.

[14]Supported by the Leverhulme Trust.

[15]Permanent address: Universitat de Barcelona, 08208 Barcelona, Spain.

[16]Supported by Bundesministerium für Bildung und Forschung, Germany.

[17]Supported by the Direction des Sciences de la Matière, C.E.A.

[18]Supported by the Austrian Ministry for Science and Transport.

[19]Now at SAP AG, 69185 Walldorf, Germany

[20]Now at Groupe d' Astroparticules de Montpellier, Université de Montpellier II, 34095 Montpellier, France.

[21]Now at BNP Paribas, 60325 Frankfurt am Mainz, Germany

[22]Supported by the US Department of Energy, grant DE-FG03-92ER40689.

[23]Now at Institut Inter-universitaire des hautes Energies (IIHE), CP 230, Université Libre de Bruxelles, 1050 Bruxelles, Belgique

[24]Also at Dipartimento di Fisica e Tecnologie Relative, Università di Palermo, Palermo, Italy.

[25]Deceased.

[26]Now at SLAC, Stanford, CA 94309, U.S.A

[27]Now at IWR, Forschungzentrum Karlsruhe, Postfach 3640, 76021 Karlsruhe, Germany

[28]Research Fellow of the Belgium FNRS

[29]Research Associate of the Belgium FNRS

[30]Now at Liverpool University, Liverpool L69 7ZE, United Kingdom

[31]Supported by the Federal Office for Scientific, Technical and Cultural Affairs through the Interuniversity Attraction Pole P5/27

[32]Now at INP, Cracow, Poland

[33]Now at Centre de Physique des Particules de Marseille, Univ. Méditerannée, F-13288 Marseille, France.

1 Introduction

In this letter, the results of the ALEPH searches for particles predicted by supersymmetry are combined to set an absolute lower limit on the mass of the lightest supersymmetric particle (LSP). This limit is obtained within the framework of the Minimal Supersymmetric extension of the Standard Model (MSSM) [1] with R-parity conservation and under the assumption that the lightest neutralino χ_1^0 is the LSP. Furthermore, the assumption of universal gaugino and sfermion mass terms at the GUT scale is made. The notations and conventions for the MSSM parameters are those given in Ref. [2].

To obtain the results presented here, the published searches for charginos and neutralinos [2, 3] have been extended to include data taken during the year 2000, at centre-of-mass energies between 202 and 209 GeV. These searches have been supplemented by specific analyses to cover final states not considered previously. The searches for selectrons, which have already been published in Ref. [4], have been optimized to increase their sensitivity in the chargino-sneutrino *corridor*, where the LSP mass limit is set [2]. The published results on searches for Higgs bosons [5] as well as for charginos accompanied by hard initial state radiation [6] have also been included to derive the LSP mass limit.

The masses of charginos and neutralinos are fully determined by the universal gaugino mass $m_{1/2}$, the Higgs-mixing mass term μ and $\tan\beta$, the ratio of vacuum expectation values of the two Higgs doublets. However, both the production cross sections and the decay branching ratios depend on the sfermion mass spectrum, which in turn depends on the universal sfermion mass m_0. In this letter, and unless otherwise specified, the effects of Yukawa couplings in the renormalization group equations used to derive the sfermion masses at the electroweak scale are neglected. Chargino (neutralino) pair production involves the exchange of a sneutrino (selectron) in the t channel, with destructive (constructive) interference with the s-channel diagram. Similarly, the decays into a neutralino and a fermion pair involve slepton and squark exchange in addition to W/Z exchange. If mixing effects in the sfermion sector are neglected, as was done in Refs. [2, 3], the lower limit on the mass of the LSP depends solely on the interplay of four parameters, m_0, $m_{1/2}$, μ and $\tan\beta$.

Mixing effects in the sfermion sector are proportional to the corresponding fermion mass m_{f} via off-diagonal terms $m_{\mathrm{f}}\, a_{\mathrm{f}}$ in the sfermion mass matrices, with $a_{\mathrm{f}} = A_{\mathrm{f}} - \mu\tan\beta$ for down-type squarks and for sleptons, and $a_{\mathrm{f}} = A_{\mathrm{f}} - \mu\cot\beta$ for up-type squarks, where A_{f} is the trilinear Higgs-sfermion coupling. These effects can therefore become important for the third generation, while they are in practice negligible for the other two generations. In particular, a large mixing in the stau sector can cause the lighter stau $\tilde{\tau}_1$ to be light enough to affect the decay patterns of charginos and neutralinos. The branching ratios of decay topologies that include τ's increase in this case, and can even dominate if the two-body decays $\chi^{\pm} \to \tilde{\tau}_1^{\pm}\nu_\tau$ and $\chi_2^0 \to \tilde{\tau}_1^{\pm}\tau^{\mp}$ are allowed kinematically.

This possibility, which affects the sensitivity of the existing searches, and consequently the lower limit derived on the mass of the LSP, is studied in this letter for the full range

of mixing angles φ_τ in the stau sector. The relation between A_τ and φ_τ is given by:

$$A_\tau = \mu \tan\beta \; - \; \frac{1}{2}\tan(2\varphi_\tau)\left(\frac{m^2_{\tilde{\tau}_R} - m^2_{\tilde{\tau}_L}}{m_\tau}\right),$$

where $m_{\tilde{\tau}_R}$ and $m_{\tilde{\tau}_L}$ are the supersymmetry-breaking mass terms associated with the two tau chirality states. The no-mixing case, for which $\tilde{\tau}_1 = \tilde{\tau}_R$, corresponds to $\varphi_\tau = 0$, such that the relation $A_\tau = \mu \tan\beta$ is fulfilled. The full range of A_τ is covered if φ_τ is varied between -45° and 45°.

Three new analyses have been developed to address the above mentioned decays for different values of the $\tilde{\tau}_1$-χ^0_1 mass difference, Δm:

- a search for $e^+e^- \to \chi^+\chi^- \to \tilde{\tau}^+_1\nu_\tau \; \tilde{\tau}^-_1\bar{\nu}_\tau \to \tau^+\nu_\tau\chi^0_1 \; \tau^-\bar{\nu}_\tau\chi^0_1$, leading to an acoplanar pair of taus in the final state, appropriate for large Δm values;
- a search for $e^+e^- \to \chi^0_j\chi^0_1 \to \tilde{\tau}_1\tau \; \chi^0_1 \to \tau\chi^0_1\tau \; \chi^0_1$ (with j=2,3,4) leading to a final state with one or two detectable taus, depending on the value of Δm;
- a search for $e^+e^- \to \chi^0_j\chi^0_2 \to \tilde{\tau}_1\tau \; \tilde{\tau}_1\tau \to \tau\tau\chi^0_1 \; \tau\tau\chi^0_1$ (with j = 2,3,4) leading to a final state with two or four detectable taus, depending on the value of Δm.

The last two analyses have been developed in particular to cover the region of mass degeneracy between the lighter stau and the LSP in the small m_0 region of the MSSM parameter space, where the neutralino production cross sections are large. For larger m_0 values, the search for charginos accompanied by hard initial state radiation (ISR), as developed in Ref. [6], is applied in addition.

In this letter, stops and sbottoms are assumed to be too heavy to affect the decay pattern of charginos and neutralinos. In the MSSM interpretation of the results, the trilinear couplings A_t and A_b are set to their no-mixing values. However, mixing in the stop and sbottom sector is appropriately taken into account in the interpretation of Higgs boson searches.

This letter is organized as follows. The ALEPH detector and the data used in the analyses are briefly described in Section 2. The update of standard chargino and neutralino searches to include the data from the year 2000, the optimization of the selectron analysis, and the specific selections developed to study the effects of stau mixing are presented in Section 3. The interpretation of results without and with stau mixing is given in Section 4, and the interpretation within the more constrained framework of minimal supergravity (mSUGRA) is presented in Section 5.

All limits reported in this letter are given at the 95% confidence level.

2 The ALEPH detector and the data sample

A thorough description of the ALEPH detector and of its performance can be found in Refs. [7, 8]. Only a brief summary is given here. Charged particle tracking, down to 16° relative to the beam axis, is achieved by means of a silicon vertex detector, a cylindrical drift chamber, and a large time projection chamber, all immersed in a 1.5 T magnetic field provided by a superconducting solenoidal coil. Hermetic calorimetric coverage, down to polar angles of 34 mrad, is achieved by means of a highly granular electromagnetic calorimeter (ECAL), dedicated low angle luminosity monitors, and an iron return yoke instrumented to act as a hadron calorimeter (HCAL). The ECAL is used to identify electrons and photons by the characteristic longitudinal and transverse developments of the associated showers, and is supplemented for low momentum electrons by a measurement of the specific energy loss through ionization in the TPC. The HCAL provides a measurement of the hadronic energy and, together with external muon chambers, efficient identification of muons by their characteristic penetration pattern.

Global event quantities such as total energy, transverse momentum, or missing energy are determined using an energy-flow algorithm which combines all the above measurements into charged particles (electrons, muons, charged hadrons), photons and neutral hadrons. These are the basic objects used in the selections presented in this letter.

The data used for the analyses entering the present combination were collected at centre-of-mass energies ranging from 183 to 209 GeV. The corresponding integrated luminosities are given in Table 1, together with the references where the relevant results are published.

Table 1: Integrated luminosities collected between 1997 and 2000, average centre-of-mass energies, and data samples used in the analyses mentioned in the text.

Year	1997	1998	1999				2000		
$\sqrt{s}$ (GeV)	182.7	188.6	191.6	195.5	199.5	201.6	205.2	206.6	208.0
$\mathcal{L}$ (pb^{-1})	56.8	173.6	28.9	79.8	86.2	42.0	75.3	122.6	9.4
$\mathrm{e^+e^-} \to \chi^+\chi^-$	Ref. [2]	Ref. [3]					This letter		
$\mathrm{e^+e^-} \to \chi^+\chi^-\gamma$	Ref. [6]								
$\mathrm{e^+e^-} \to \chi_i^0\chi_j^0$	Ref. [2]	Ref. [3]					This letter		
$\mathrm{e^+e^-} \to \tilde{\ell}^+\tilde{\ell}^-$	Ref. [4] and this letter								
$\mathrm{e^+e^-} \to \mathrm{hZ}$	Ref. [5]								
Specific searches (for decays into staus)									
$\chi^\pm \to \tilde{\tau}_1^\pm\nu_\tau$	–	This letter							
$\chi_2^0 \to \tilde{\tau}_1^\mp\tau^\pm$	–	This letter							

3 Event Selections

The selection criteria described below have been optimized using the $\bar{N}_{95}$ prescription [9], which consists in minimizing the upper limit on the signal cross section expected in the absence of signal processes. This has been done by applying all selections to fully simulated Standard Model background samples, generated as described in Ref. [2] for $e^+e^- \to f\bar{f}$, WW, ZZ, Zee, Weν, Z$\nu\bar{\nu}$, and for $\gamma\gamma$ interactions. The simulation of supersymmetry signal processes has been performed with SUSYGEN [10].

3.1 Update of chargino and neutralino searches

Chargino and neutralino pair production, $e^+e^- \to \chi^+\chi^-$ and $e^+e^- \to \chi_i^0\chi_j^0$, has already been searched for in the ALEPH data up to centre-of-mass energies of 202 GeV [2, 3]. Up to twenty selection algorithms had been designed to cover different decay channels as well as different regions of mass difference ΔM between the produced chargino or the heavier neutralino and the LSP. They address final states with four jets, two jets and a lepton, acoplanar jets or acoplanar leptons, all accompanied by missing energy. The same searches have been applied to the data collected in the year 2000 with an appropriate adjustment of the selection criteria according to the increased centre-of-mass energy.

In all cases, the numbers of events observed are in agreement with those expected from Standard Model background sources, dominated by $\gamma\gamma$ interactions for small ΔM and by four-fermion processes (mostly WW and Weν production) for large ΔM. These numbers are displayed in Table 2 for the combination of analyses optimal for large m_0 values, for which only three-body decays occur, and small m_0 values, for which leptonic branching fractions are enhanced. Because of ΔM-dependent sliding cuts, each event contributes to only a limited range of ΔM values.

Table 2: Numbers of events observed in the year 2000 data ($N_{\rm obs}$) and expected from Standard Model background sources ($N_{\rm exp}$) in standard chargino and neutralino searches.

Chargino searches				Neutralino searches			
Large m_0		Small m_0		Large m_0		Small m_0	
$N_{\rm obs}$	$N_{\rm exp}$	$N_{\rm obs}$	$N_{\rm exp}$	$N_{\rm obs}$	$N_{\rm exp}$	$N_{\rm obs}$	$N_{\rm exp}$
11	11.1	35	32.0	1	1.5	82	73.5

3.2 Optimization of the selectron search

The published searches for selectrons have been optimized to increase the sensitivity for the LSP mass limit. In Ref. [4], the selectron selection uses the momenta of the reconstructed charged particle tracks to estimate the electron energies. This choice was not critical because, at very large ΔM, *i.e.*, where the selectron mass limit is set, the signal

and the main background process ($W^+W^- \to e^+\nu\ e^-\bar{\nu}$) have very similar characteristics. In particular, the amount of bremsstrahlung energy lost by the electrons is similar.

For intermediate values of ΔM, where the LSP mass limit is set, however, the signal electrons are, on average, less energetic and radiate less energy. The discriminating power of the selection is therefore increased by including the neutral energy in a cone around the charged particle in the lepton energy estimate. The optimized selection has been applied to the data collected in 1999 and 2000. Before applying mass-dependent sliding cuts, the event numbers are identical to the ones reported in Ref. [4].

3.3 Search for $\chi^+\chi^- \to \tilde{\tau}_1^+\nu_\tau\ \tilde{\tau}_1^-\bar{\nu}_\tau \to \tau^+\nu_\tau\chi_1^0\ \tau^-\bar{\nu}_\tau\chi_1^0$

Chargino two-body decays to a stau and a neutrino can be significant for small m_0 values or large mixing in the stau sector. For large values of Δm, the mass difference between the stau and the lightest neutralino, the final state consists of an acoplanar pair of taus. The search for acoplanar tau pairs described in Ref. [4] has therefore been used. The efficiency depends primarily on Δm, while the mass difference ΔM between the chargino and the lightest neutralino has less impact. The efficiency for signal events is shown in Fig.1a as a function of Δm, for several values of ΔM. As in Ref. [4], the final selection involves mass dependent cuts on the visible momenta of the taus. A comparison between the number of candidate events and the Standard Model expectation is presented in Fig. 1b as a function of Δm (for $\Delta M = 50\,\mathrm{GeV/c^2}$).

For smaller values of Δm, the taus from the stau decays are too soft to be detected and the above final state becomes invisible. The analysis has therefore been supplemented with a search for an energetic ISR photon produced in association with the invisibly decaying chargino pair, as described in Ref. [6]. For $\Delta m = 2\,\mathrm{GeV/c^2}$, the efficiency of this selection ranges from 0.5% to 2.3%, for m_{χ^+} between 90 and $60\,\mathrm{GeV/c^2}$.

3.4 Dedicated searches for neutralino decays into staus

For small m_0 and substantial mixing in the stau sector, two-body decays of heavier neutralinos, $\chi_j^0 \to \tilde{\tau}\tau \to \tau\tau\chi_1^0$, lead to at least one tau with enough momentum to be detected even for very small Δm. These decays are exploited here to supplement the search for invisible charginos with ISR.

3.4.1 Search for $\chi_j^0\chi_1^0 \to \tilde{\tau}\tau\chi_1^0 \to \tau\chi_1^0\tau\chi_1^0$

The associated neutralino production leads to final states with one (for small Δm) or two (for larger Δm) visible taus. Analyses have been developed to cover both final states and are referred to as single-tau and asymmetric tau-pair searches in the following. The tau identification criteria are given in Ref. [11].

The single-tau selection is developed in analogy to the single-electron selection described as well in Ref. [11]. A search is performed for a single identified tau decay.

The visible transverse momentum of the decay products is required to be larger than $0.04\ \sqrt{s}$. Events are rejected if they contain a second identified tau with a momentum above 1 GeV/c. If the tau decay product is a single charged particle identified as an electron or a muon, the momentum of this lepton is required to be smaller than 45% of the beam energy.

The tau can be accompanied by some additional energy in the event, *i.e.*, low momentum tracks or small energy depositions in the calorimeters. This remaining energy is required to be smaller than 10 GeV, but events with no additional charged particles, likely to be due to the Weν background, are rejected. The acoplanarity angle between the directions of the identified tau and of the leading additional charged particle is required to be larger than 10° and smaller than 170°. In order to reduce the background from $\gamma\gamma$ events, it is required that no energy be detected within 12° of the beam axis, and the upper cutoff on the acoplanarity is lowered from 170° to 140° for low energy tau candidates, *i.e.,* if $E_\tau/E_{\rm beam} < 0.25$.

A parametrization of the signal efficiency is shown in Fig. 2a as a function of Δm (for $\Delta M = 46\,\mathrm{GeV/c^2}$, where ΔM is the mass difference between the heavier and the lightest neutralino). Because of the cutoff on the remaining energy, the efficiency decreases with increasing Δm. To weaken this effect, this analysis is combined with an asymmetric tau-pair search. The selection is again based on the stau pair production search [4]. However, the final sliding cuts on the momenta of the taus have been optimized for the new decay kinematics. To select asymmetric tau pairs, the momentum of the second tau is required to be lower than a Δm-dependent cutoff value. Over the Δm range between 2 and $8\,\mathrm{GeV/c^2}$, this cutoff value increases from 6.5 to $20.4\,\mathrm{GeV}/c$. In addition, an upper cut on the momentum of the leading tau is applied, depending on both Δm and the momentum of the second tau. The contribution of this selection to the signal efficiency is also shown in Fig. 2a. The efficiencies of both selections have been found to be rather insensitive to the exact ΔM value, *e.g.,* the relative efficiency variations are below 10% if ΔM is changed from 35 to $46\,\mathrm{GeV/c^2}$.

The combination of the single-tau and asymmetric tau-pair analyses covers the small-Δm range down to values close to the tau mass. For smaller mass differences, staus cannot decay into $\tau\chi_1^0$ and become long-lived. This configuration is efficiently covered by the search for stable heavy charged particles [12].

3.4.2 Search for $\chi_{\rm j}^0\chi_2^0 \to \tilde\tau\tau\ \tilde\tau\tau \to \tau\tau\chi_1^0\ \tau\tau\chi_1^0$

If χ_2^0 pair production or associated production of a heavier neutralino with χ_2^0 are kinematically accessible, four-tau final states are expected, in which at least two taus are visible. This clear signature can be efficiently selected with the search presented in Ref. [12], developed in the framework of gauge-mediated supersymmetry breaking studies. When applied to χ_2^0 pair production, the efficiency of the four-tau selection is of the order of 40 to 50% (Fig. 2a) in the whole range of Δm values from 2 to $20\,\mathrm{GeV}/c^2$. The efficiency is found to be essentially independent of ΔM, for values in the range between 30 and $45\,\mathrm{GeV/c^2}$.

3.4.3 Results

In the data collected between 1998 and 2000, 46 single-tau events are observed, to be compared with an expectation of 44.7 events from background sources. Good agreement is also found for the asymmetric tau-pair analysis. A comparison between the number of events observed and the expectation from Standard Model backgrounds is shown in Fig.2b. In the same data sample, 22 four-tau events are observed, in agreement with the expectation of 16.5 events from background sources. For the three analyses, the background is dominated by WW and Weν events, with a smaller contribution from $\gamma\gamma \to \tau\tau$.

4 Interpretation of the results

The numbers and properties of the events in all analyses are in good agreement with the expectations from the Standard Model. The negative result of the searches can be translated into upper limits on the chargino and neutralino production cross sections. To derive these limits, the method of Ref. [13] is used whenever background subtraction is performed. The procedure is unchanged with respect to Ref. [3] for the updated chargino and neutralino searches. For the analyses based on the acoplanar tau-pair selection, the dominant WW background is subtracted. The new dedicated searches for neutralinos decaying into staus suffer from a significant background from Weν, Zee and $\gamma\gamma \to \tau\tau$ which is also subtracted.

The main systematic errors affecting the updated analyses, related to the simulation of the energy flow reconstruction and of the lepton identification, are unchanged with respect to Ref. [14]. The efficiencies of the dedicated searches for neutralinos are in addition affected by a relative systematic uncertainty of 10% associated with the τ identification. In the following, the systematic uncertainties are included in the derivation of the results according to the method proposed in Ref. [15].

4.1 Constraints on the MSSM parameters

The upper limits on the production cross sections of charginos and neutralinos can be used to constrain the space of the relevant MSSM parameters. The production cross sections and the decay branching ratios have been calculated, here and in the following, using the programme MSMLIB [16].

The domains excluded in the (μ, M_2) plane are shown for $\tan\beta = \sqrt{2}$ in Figs. 3a and 3b for $\mu < 0$ and $\mu > 0$, respectively, assuming that all scalars are heavy enough ($m_0 = 500\,\mathrm{GeV/c^2}$) to play a negligible rôle in the phenomenology of charginos and neutralinos. The electroweak scale value M_2 of the SU(2) gaugino mass term is related by $M_2 \approx 0.81 m_{1/2}$ to its value at the GUT scale. For small $\tan\beta$ and small negative μ, the domain excluded by chargino searches is extended by neutralino searches.

These exclusions can be translated into lower limits on chargino and neutralino masses. Examples of these results are presented in Figs. 3c and 3d. The kinematic limit is closely approached for both chargino and associated neutralino production, except at large M_2, where the searches lose sensitivity because of the small ΔM values predicted by the model. The case of charginos at small ΔM has been studied in Ref. [6], where a mass lower limit of $88\,\mathrm{GeV/c^2}$ is obtained for large m_0. For $\tan\beta = \sqrt{2}$ and negative μ, the chargino mass limit derived indirectly from neutralino searches extends beyond the kinematic limit of chargino pair production by up to $6\,\mathrm{GeV/c^2}$.

4.2 The LSP mass lower limit in the case of no stau mixing

The lower limit on the mass of the LSP derived from chargino and neutralino searches for $m_0 = 500\,\mathrm{GeV/c^2}$ is shown as a function of $\tan\beta$ in Fig. 4. For this m_0 value, the smallest allowed value for the mass of the LSP is $39.6\,\mathrm{GeV/c^2}$. It is found for $\tan\beta = 1$, $M_2 \simeq 67\,\mathrm{GeV/c^2}$ and $\mu \simeq -78\,\mathrm{GeV/c^2}$. The mass lower limit derived from chargino searches alone is $38\,\mathrm{GeV/c^2}$. For smaller m_0, the loss of sensitivity of chargino searches is recovered by slepton searches, as discussed in Ref. [2]. A scan performed over the relevant parameter space shows that the lower limit on the mass of the LSP, obtained for $\tan\beta = 1$ and large m_0, holds for any value of m_0.

Higgs boson searches have been included to further constrain the LSP mass, as discussed in Ref. [3]. The result is shown in Fig. 4. The lower limit on the mass of the LSP is improved for $\tan\beta$ values smaller than 3.9, in such a way that the absolute lower limit is now found at large $\tan\beta$ and large negative μ. For $\tan\beta = 35$ the result is $43.1\,\mathrm{GeV/c^2}$, independent of m_0. This limit is determined by the result of selectron searches in the *corridor* of sneutrino-chargino mass degeneracy. The situation in the $(m_0, m_{1/2})$ plane is illustrated in Fig. 5a for $\tan\beta = 35$ and $\mu = -1000\,\mathrm{GeV/c^2}$, where the regions excluded by searches for three-body chargino decays, for two-body chargino decays via sneutrinos, for selectrons and for staus are shown.

Higgs boson searches cover a larger fraction of the corridor as $\tan\beta$ decreases. As a result, the LSP mass limit moves into the region of large m_0 for $\tan\beta < 3.2$, and is set by the chargino searches. The results obtained using the Higgs boson searches depend on the value chosen for the top quark mass, m_t, on the maximum m_0 considered and on the theoretical uncertainty from the calculation of radiative corrections to the Higgs boson mass. This last uncertainty is conservatively taken into account by increasing the predicted Higgs boson mass by $2\,\mathrm{GeV/c^2}$. For $m_t = 175\ \mathrm{GeV/c^2}$ and $m_0 \leq 1\,\mathrm{TeV/c^2}$, the lower limit on the mass of the LSP for $\tan\beta < 3.2$ is $49.3\,\mathrm{GeV/c^2}$. For $m_t = 180\,\mathrm{GeV/c^2}$ and $m_0 \leq 2\,\mathrm{TeV/c^2}$, this limit is reduced to $45.5\,\mathrm{GeV/c^2}$ except for a narrow region of $\tan\beta$ around 1.0. This region is however excluded if the LEP combined limit for the Higgs boson mass [17] is used instead of the sole ALEPH limit.

4.3 The impact of stau mixing on the LSP mass lower limit

As mentioned in Section 1, stau mixing may significantly affect the decay pattern of charginos and neutralinos. It has therefore been investigated how the lower limit on the mass of the LSP presented in Section 4.2 is changed if mixing in the stau sector is allowed for. In addition to the analyses considered in Section 4.2, the searches for chargino decays via staus as well as nearly invisible chargino decays accompanied by hard ISR, and the dedicated searches for neutralino decays into staus, have been included.

The effects of stau mixing are illustrated in the gaugino region ($\mu = -1000\,\mathrm{GeV/c^2}$) for $\tan\beta = 35$ in Figs. 5a-d. The excluded regions in the $(m_0, m_{1/2})$ plane are shown for four values of the stau mixing angle (φ_τ =0, 30, 35 and 40 degrees).

With increasing stau mixing, the leptonic decay channels of the charginos become more important. When the lighter stau gets lighter than the chargino, the $\tilde{\tau}\nu$ decay mode of the chargino dominates, and a significant region of the parameter space is excluded by searches for that decay channel (region III in Fig. 5). For mixing angles near 35°, the limit on the mass of the LSP is determined by direct stau searches and chargino searches via decays into staus.

For large enough mixing angles the stau mass approaches the mass of the LSP and direct stau decays into the LSP lose sensitivity, due to the small mass difference Δm involved. A new uncovered corridor, the stau-LSP corridor, appears. The dedicated searches for neutralinos decaying into staus and for charginos accompanied by hard ISR allow sensitivity to be recovered in that region. The relative importance of these analyses depends on the location of the stau-LSP corridor in the $(m_0, m_{1/2})$ plane. For mixing angles near 40°, the neutralino analyses protect the lower limit on the LSP mass. For larger mixing angles, the corridor shifts towards larger m_0 (for fixed $m_{1/2}$), so that the chargino cross section is large enough for that region to be excluded by using the search for charginos with hard ISR, despite the small efficiency of the selection. The interplay of the different analyses for large mixing angles is shown in Figs. 5c and 5d.

In order to extract the LSP mass lower limit in the presence of stau mixing, a scan over the parameter range

$$\begin{aligned} 1 < \ & \tan\beta \ < 50, \\ |\mu| \ < \ & 20\,\mathrm{TeV/c^2}, \end{aligned}$$

and the full range of stau mixing angles

$$-45^\circ \ < \ \varphi_\tau \ < \ 45^\circ$$

has been performed. The results for the LSP mass limit as a function of $|\tan\varphi_\tau|$ are shown in Fig. 6a. The limit is shown for various values of $\tan\beta$ as well as for the scan over the full $\tan\beta$ range considered. No large differences for the LSP mass lower limit have been found between positive and negative mixing angles. The only significant differences appear for large $\tan\beta$ values, where for negative mixing angles the LSP mass lower limit has been found to be up to $0.4\,\mathrm{GeV/c^2}$ higher than for the corresponding positive angles.

The LSP mass limit is relatively stable for large $\tan\beta$ values and the limit found in the non-mixing case is only slightly degraded. A minimum, corresponding to an LSP mass value of $42.4\,\mathrm{GeV/c^2}$, is found for $\tan\varphi_\tau$ values around 0.96 in the region of large negative μ. For these extreme mixing angles, where the stau-LSP corridor appears, the LSP lower mass limit is stabilized by the dedicated neutralino analyses and by the search for invisibly decaying charginos accompanied by hard photons.

In the region of small $\tan\beta$ the LSP mass lower limit is weaker and is found for μ values in the range $-100\,\mathrm{GeV/c^2} < \mu < -60\,\mathrm{GeV/c^2}$, a region where the chargino production cross sections are small. In addition to a minimum for $\tan\varphi_\tau$ values around 0.8, a second minimum is found for extreme mixing angles ($\varphi_\tau \sim 44.8°$). Besides chargino production, stau-pair production is the only SUSY process with a significant cross section in that region. However, due to the small Δm value, it cannot be exploited to improve the mass limit. The absolute LSP mass lower limit is determined by the chargino search with hard ISR and is found to be $29.7\,\mathrm{GeV/c^2}$ at $\tan\beta \sim 1.1$, $\mu \sim -80\,\mathrm{GeV/c^2}$, $m_0 \sim 375\,\mathrm{GeV/c^2}$ and $\varphi_\tau = 44.85°$, which corresponds to $A_\tau \sim -80\,\mathrm{TeV/c^2}$.

The LSP mass lower limit is shown in Fig. 6b as a function of $\tan\beta$. As in the no-mixing case, the standard neutralino searches can be applied to improve the limit in the small $\tan\beta$ region. In a detailed scan it has been verified that in the region of intermediate mixing angles, *i.e.,* $\tan\varphi_\tau < 0.9$, all LSP masses smaller than $36.6\,\mathrm{GeV/c^2}$ can be excluded by the standard neutralino searches. Due to the tiny cross sections for associated neutralino production these analyses do not improve the LSP mass lower limit in the regions of extreme and unnaturally large A_τ values. If A_τ is restricted to $|A_\tau| < 20\,\mathrm{TeV/c^2}$ the limit of $36.6\,\mathrm{GeV/c^2}$ holds over the full parameter space.

The low $\tan\beta$ region can further be covered by Higgs boson searches. As in Ref. [18], the range of trilinear couplings ($|A_\mathrm{t}|$ and, here, $|A_\tau|$) has been restricted to a maximum of $4\,\mathrm{TeV/c^2}$. The constraints obtained in the no-mixing case are found to hold if stau mixing is taken into account. The LSP mass lower limit with stau mixing is therefore the one obtained at large $\tan\beta$, namely $42.4\,\mathrm{GeV/c^2}$.

A summary of the results obtained for the LSP mass lower limit is given in Table 3. As discussed in Ref. [3], these limits are affected by theoretical uncertainties of the order of a $\mathrm{GeV/c^2}$.

The Delphi experiment at LEP [19] has set a LSP mass limit of $46\,\mathrm{GeV/c^2}$ using Higgs boson searches and assuming no stau mixing. For $\tan\beta > 3$, a limit of $45.5\,\mathrm{GeV/c^2}$ is obtained for $|A_\mathrm{t}|$ and $|A_\tau|$ smaller than $1\,\mathrm{TeV/c^2}$. For $\tan\beta > 2$, a limit of $39\,\mathrm{GeV/c^2}$ is set for any A_τ and assuming no mixing in the stop sector.

4.4 Interpretation in Minimal Supergravity

The interpretation in the framework of minimal supergravity presented in Refs. [2, 3] has been updated with the final results of the searches for charginos and neutralinos presented in the previous sections, and those for sleptons [4] and neutral Higgs bosons [5]. In particular, the inclusion of the specific searches described in Sections 3.3 and 3.4 allows

Table 3: Summary of the LSP mass lower limits in the MSSM. The Higgs constraints are obtained under the assumptions $m_t = 175\,\mathrm{GeV/c^2}$, $m_0 \leq 1\,\mathrm{TeV/c^2}$ and $|A_t| \leq 4\,\mathrm{TeV/c^2}$.

Stau mixing	$\tan\beta$ range	Higgs searches	LSP mass lower limit
$\varphi_\tau = 0.$	> 1.0	none	$39.6\,\mathrm{GeV/c^2}$
	> 1.0	included	$43.1\,\mathrm{GeV/c^2}$
Any φ_τ	> 1.0	none	$29.7\ \mathrm{GeV/c^2}$
$\lvert A_\tau\rvert < 20\,\mathrm{TeV/c^2}$	> 1.0	none	$36.6\ \mathrm{GeV/c^2}$
$\lvert A_\tau\rvert < 4\,\mathrm{TeV/c^2}$	> 1.0	included	$42.4\,\mathrm{GeV/c^2}$

the condition $m_{\tilde{\tau}} - m_{\chi_1^0} > 5\,\mathrm{GeV/c^2}$, needed in Refs. [2, 3] to avoid the stau-LSP corridor, to be relaxed. In this analysis, the full renormalization group equations, including Yukawa couplings, have been used to derive the sfermion masses at the electroweak scale.

The interplay among the different searches is shown in Fig. 7 as exclusion domains in the $(m_0, m_{1/2})$ plane for $\tan\beta = 10$ and 30, for $\mu < 0$ and $\mu > 0$, and for $A_0 = 0$, where A_0 is the universal trilinear coupling at the GUT scale. The top quark mass has been set to $175\,\mathrm{GeV/c^2}$. The extent of the regions covered by the searches for Higgs bosons in the hZ channel decreases as a function of $\tan\beta$ and saturates for $\tan\beta \gtrsim 30$. Here too, a theoretical uncertainty of $2\,\mathrm{GeV/c^2}$ for the Higgs boson mass has been taken into account.

The lower limit on the LSP mass is shown in Fig. 8 as a function of $\tan\beta$ for $A_0 = 0$ and both signs of μ. The lowest allowed value for the LSP mass is found at large values of m_0, typically 700–800 $\mathrm{GeV/c^2}$ for large $\tan\beta$. Altogether, an LSP mass lower limit of $53\,\mathrm{GeV/c^2}$ is set for $A_0 = 0$. It is reached for $\tan\beta \sim 7.0$ and $\mu < 0$.

The impact of a non-vanishing A_0 value has been studied by scanning the range allowed by theoretical constraints and by stop searches [20]. The lower limit on the mass of the LSP as a function of $\tan\beta$ obtained from the A_0 scan is also shown in Fig. 8. In this case the LSP mass lower limit decreases to $50\,\mathrm{GeV/c^2}$, a value reached for $\tan\beta \sim 6.5$ and $\mu < 0$.

5 Conclusions

Results of searches for charginos and neutralinos have been presented using data from the ALEPH experiment collected at centre-of-mass energies up to 209 GeV. In all topologies considered, the number of candidates observed is consistent with the background expected from Standard Model processes. Under the assumption of gaugino and sfermion mass unification, these results, together with those from slepton and Higgs boson searches, provide a lower limit on the mass of the lightest supersymmetric particle of the MSSM.

The results are summarized in Table 3. If mixing in the stau sector is neglected, the LSP mass limit is 43.1 $\mathrm{GeV/c^2}$. This limit slightly degrades to 42.4 $\mathrm{GeV/c^2}$ if stau mixing is considered. In the framework of minimal supergravity, the LSP mass limit is 50 $\mathrm{GeV/c^2}$.

Acknowledgements

It is a pleasure to congratulate our colleagues from the accelerator divisions for the outstanding operation of LEP 2, especially in its last year of running, during which the accelerator performance was pushed beyond expectation. We are indebted to the engineers and technicians at all our institutions for their contributions to the excellent performance of ALEPH. Those of us from non-member states wish to thank CERN for its hospitality and support.

References

[1] H.P. Nilles, Phys. Rep. **110** (1984) 1;
H.E. Haber and G.L. Kane, Phys. Rep. **117** (1985) 75;
S.P. Martin, in *Perspectives on supersymmetry*, Ed. G.L. Kane, World Scientific, (1998) 1-98, hep-ph/9709356.

[2] ALEPH Coll., "*Search for charginos and neutralinos in e^+e^- collisions at centre-of-mass energies near 183 GeV and constraints on the MSSM parameter space* ", Eur. Phys. J. **C11** (1999) 193.

[3] ALEPH Coll., "*Search for supersymmetric particles in e^+e^- collisions at $\sqrt{s}$, up to 202 GeV and mass limit for the lightest neutralino* ", Phys. Lett. **B499** (2001) 67.

[4] ALEPH Coll., "*Search for scalar leptons in e^+e^- collisions at centre-of-mass energies up to 209 GeV* ", Phys. Lett. **B526** (2002) 206.

[5] ALEPH Coll., "*Final results of the searches for neutral Higgs bosons in e^+e^- collisions at $\sqrt{s}$ up to 209 GeV* ", Phys. Lett. **B526** (2002) 191.

[6] ALEPH Coll., "*Search for charginos nearly mass degenerate with the lightest neutralino in e^+e^- collisions at centre-of-mass energies up to 209 GeV* ", Phys. Lett. **B533** (2002) 223.

[7] ALEPH Coll., "*ALEPH: a detector for electron-positron annihilations at LEP* ", Nucl. Instrum. and Methods **A294** (1990) 121; D. Creanza *et al.*, "*The new ALEPH silicon vertex detector* ", Nucl. Instrum. and Methods **A409** (1998) 157.

[8] ALEPH Coll., "*Performance of the ALEPH detector at LEP* ", Nucl. Instrum. and Methods **A360** (1995) 481.

[9] J.F. Grivaz and F. Le Diberder, "*Complementary analysis and acceptance optimization in new particle searches* ", LAL **92–37**(1992);
ALEPH Coll., "*Search for the standard model Higgs boson* ", Phys. Lett. **B313** (1993) 299.

[10] S. Katsanevas and P. Moravitz, Comp. Phys. Commun. **112** (1998) 227.

[11] ALEPH Coll., "*Search for sleptons in e^+e^- collisions at centre-of-mass energies up to 184 GeV* ", Phys. Lett. **B433** (1998) 176.

[12] ALEPH Coll., "*Search for gauge mediated SUSY breaking topologies in e^+e^- collisions at centre-of-mass energies up to 209 GeV* ", Eur. Phys. J. **C25** (2002) 339.

[13] D.E. Groom et al., *Review of Particle Physics*, Eur. Phys. J. **C15** (2000) 1.

[14] ALEPH Coll., "*Search for charginos and neutralinos in e^+e^- collisions at $\sqrt{s}$=161 and 172 GeV* ", Eur. Phys. J. **C2** (1998) 3.

[15] R.D. Cousins and W.L. Highland, Nucl. Instrum. and Methods **A320** (1992) 331.

[16] G. Ganis, "*MSMLIB - A collection of Fortran subroutines for calculations in supersymmetric models using R parity conservation* ",
http://home.cern.ch/ganis/MSMLIB/msmlib.html

[17] ALEPH, DELPHI, L3 and OPAL Coll., "*Search for the Standard Model Higgs boson at LEP* ", Phys. Lett. **B565** (2003) 61.

[18] ALEPH Coll., "*Search for the neutral Higgs bosons of the MSSM in e^+e^- collisions at centre-of-mass energies of 181-184 GeV* ", Phys. Lett. **B440** (1998) 419;
ALEPH Coll., "*Search for the neutral Higgs bosons of the Standard Model and the MSSM in e^+e^- collisions at $\sqrt{s}$ = 189 GeV* ", Eur. Phys. J. **C17** (2000) 223.

[19] DELPHI Coll., "*Searches for supersymmetric particles in e^+e^- collisions up to 208 GeV and interpretation of the results within the MSSM* ", CERN-EP/2003-007.

[20] ALEPH Coll., "*Search for scalar quarks in e^+e^- collisions at $\sqrt{s}$ up to 209 GeV* ", Phys. Lett. **B537** (2002) 5.

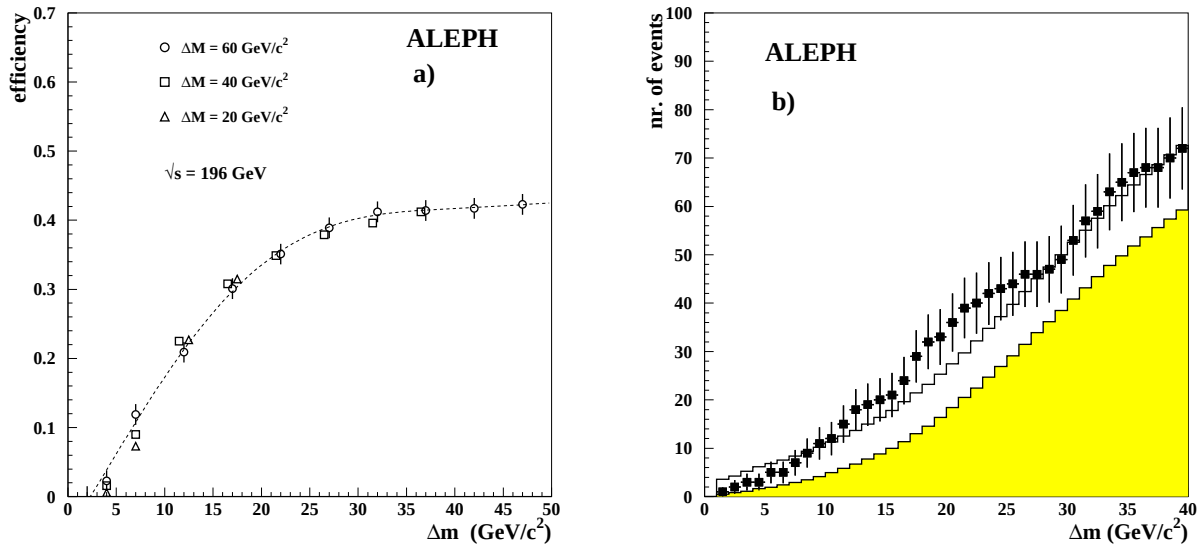

Figure 1: *a) Efficiency of the acoplanar tau-pair selection for chargino decays via staus as a function of Δm for different values of ΔM, for $m(\chi^{\pm}) = 89\,GeV/c^2$ and $\sqrt{s} = 196$ GeV. b) As a function of Δm (for $\Delta M = 50\ GeV/c^2$), comparison of the number of acoplanar tau pair candidate events (points with error bars) with the total background expectation (open histogram) after the application of the mass-dependent cuts. The contribution of the dominant WW background is represented by the shaded histogram. Each candidate event contributes to a finite Δm range, neighbouring points are therefore strongly correlated.*

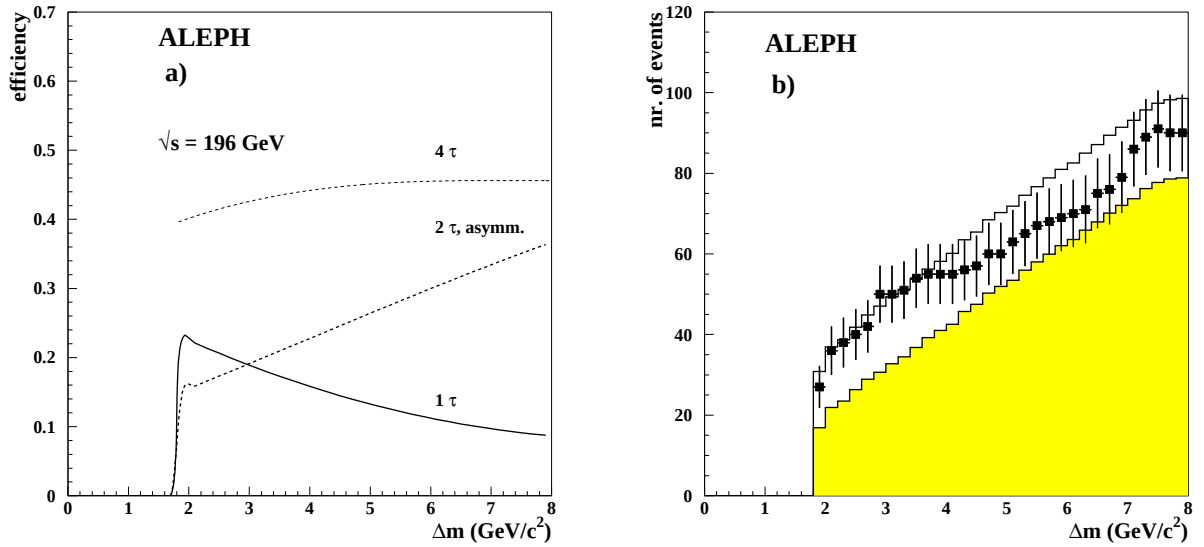

Figure 2: *a) Parametrizations of the efficiency of the single-tau, asymmetric tau-pair and four-tau analyses for $\sqrt{s} = 196\,GeV$ as a function of Δm. The neutralino masses used are $m(\chi_2^0) = 87\,GeV/c^2$ and $m(\chi_1^0) = 41\,GeV/c^2$. b) As a function of Δm, comparison of the number of tau-pair candidate events (points with error bars) with the total background expectation (open histogram). The contribution of the WW background is shown shaded. Each candidate event contributes to a finite Δm range, neighbouring points are therefore strongly correlated.*

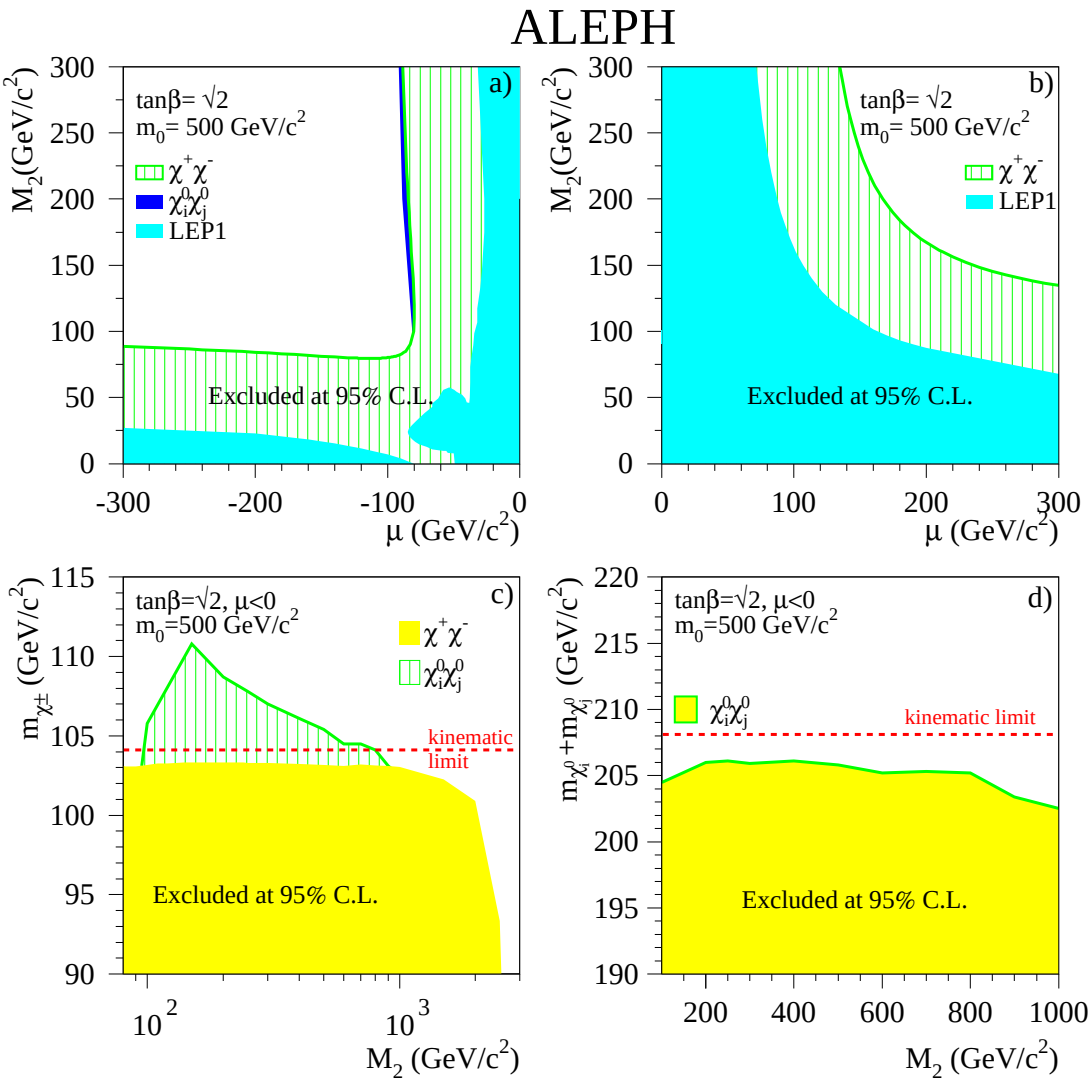

Figure 3: *Results from chargino and neutralino searches for $m_0 = 500\ GeV/c^2$ and $tan\beta = \sqrt{2}$. a) and b) Excluded domains in the (μ,M_2) plane of the MSSM for $\mu < 0$ and $\mu > 0$, respectively. c) Chargino mass lower limit as a function of M_2 for $\mu < 0$. d) Lower limit on the sum of the masses of the two neutralinos produced with the largest cross section for $\mu < 0$, as a function of M_2.*

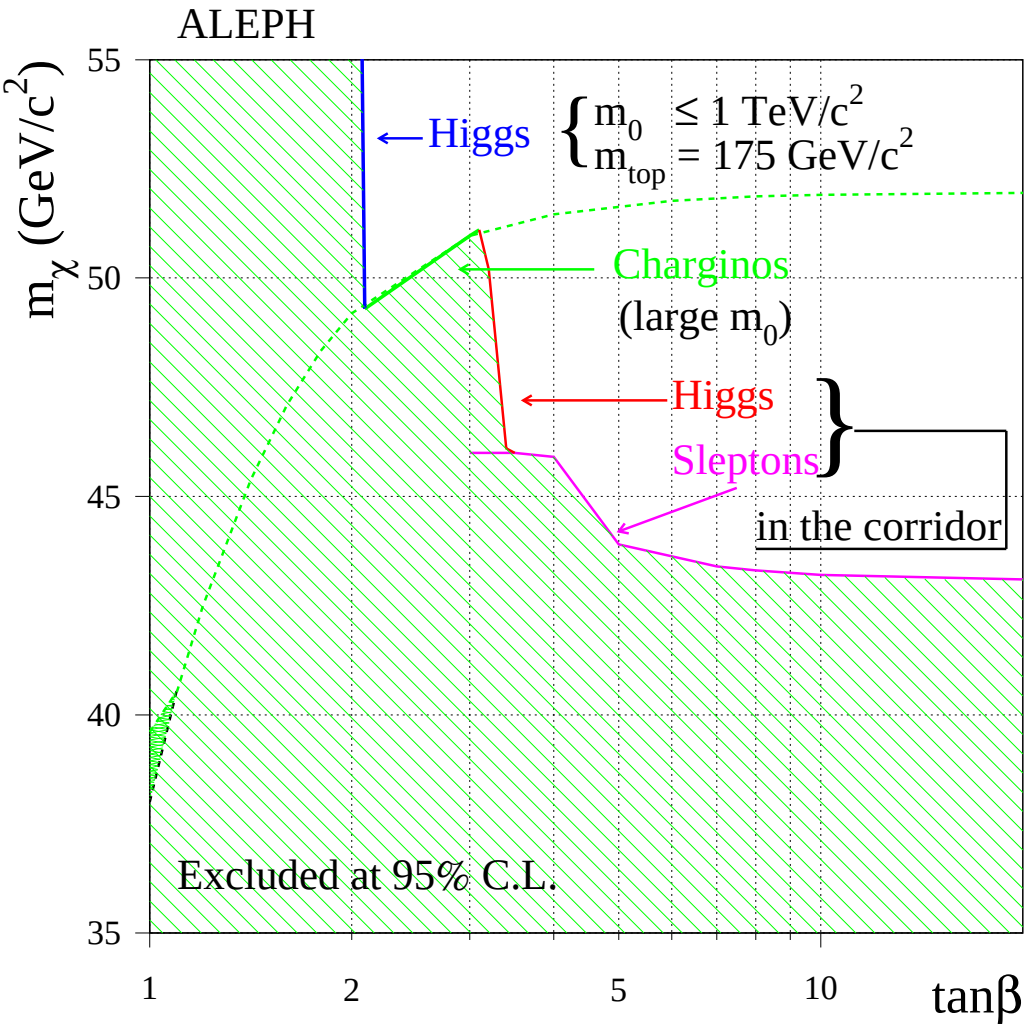

Figure 4: *The 95% C.L. lower limit on the mass of the lightest neutralino, as a function of tanβ. The dashed curve indicates the limit from chargino searches alone for $m_0 = 500$ GeV/c^2. The grey area at small tanβ shows the improvement obtained if chargino and neutralino searches are combined. The other limit curves are achieved from (right to left) slepton searches in the corridor, Higgs boson searches in the corridor, chargino searches for large sfermion masses and Higgs boson searches.*

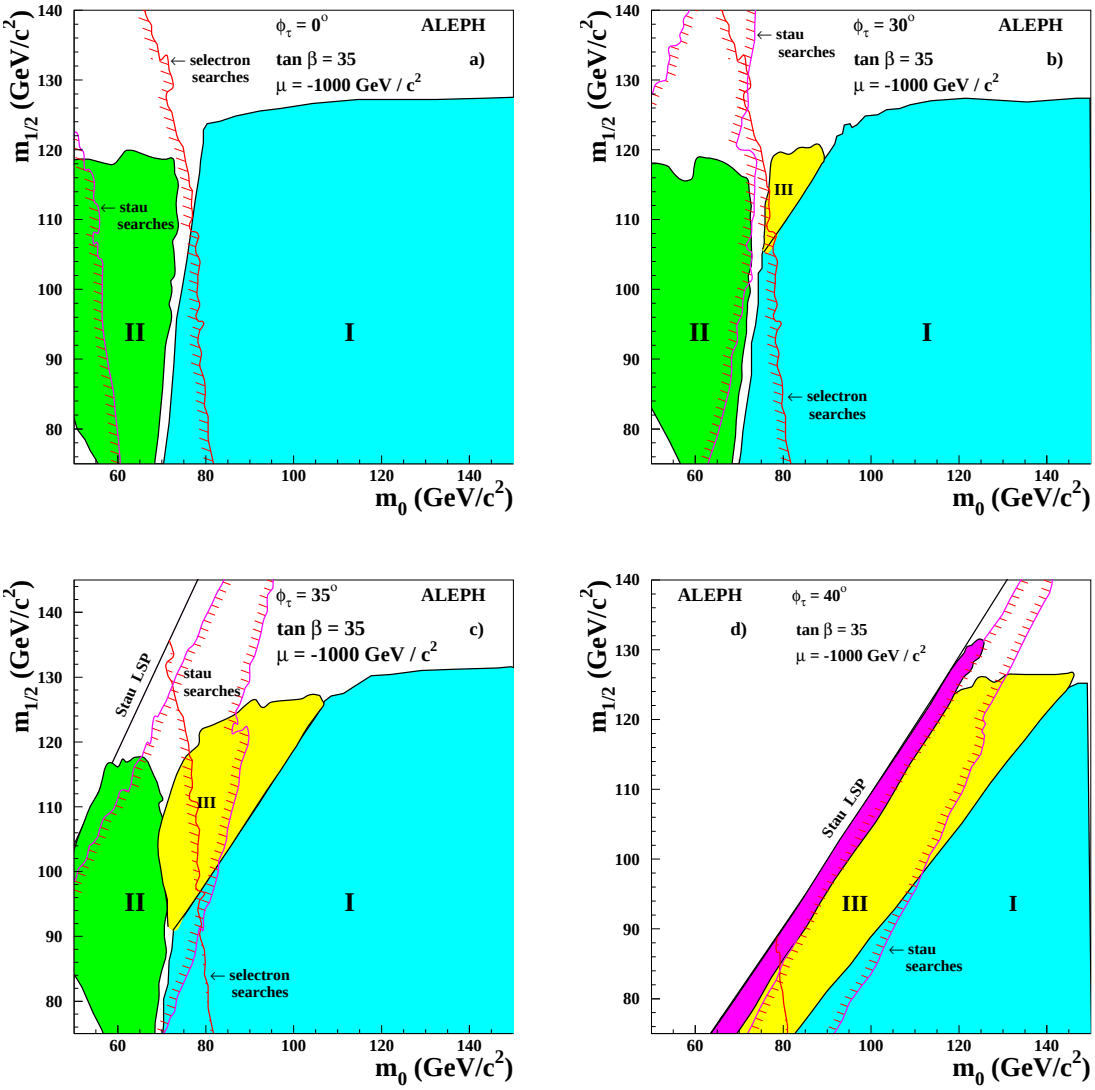

Figure 5: *Limits in the $(m_0, m_{1/2})$-plane for a point in the gaugino region (μ = -1000 GeV/c^2), for tanβ = 35, and for various stau mixing angles φ_τ. The regions marked in the plots are excluded by searches for three-body chargino decays (region I), two-body chargino decays (region II), chargino decays via staus (region III), selectron and stau searches (indicated in the plot) and by the dedicated searches for neutralinos decaying into staus and for charginos accompanied by hard ISR (region close to the stau LSP line). The regions in the upper left corner at large mixing angles are either unphysical or the $\tilde{\tau}$ is the LSP.*

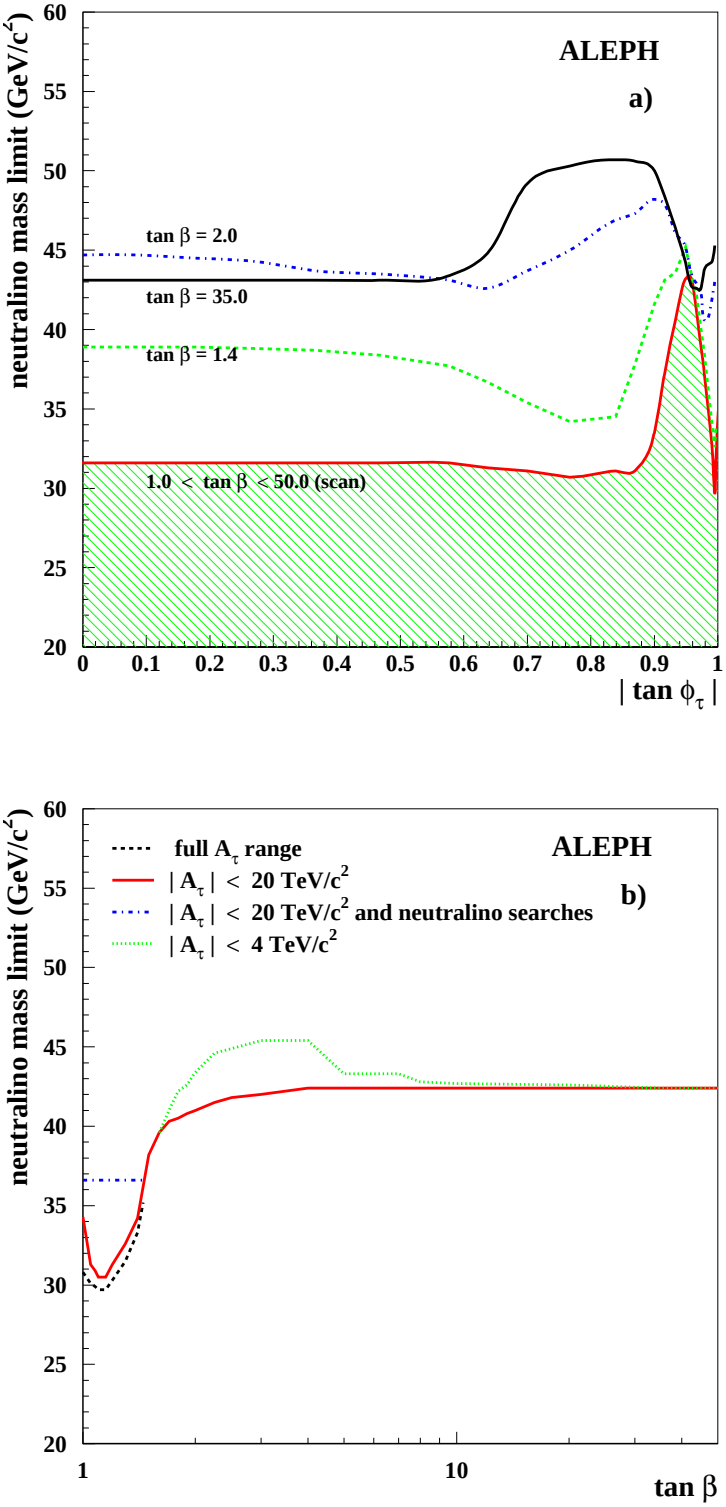

Figure 6: *Limits on the mass of the lightest neutralino as a function of (a) $|tan\varphi_\tau|$ and (b) $tan\beta$.*

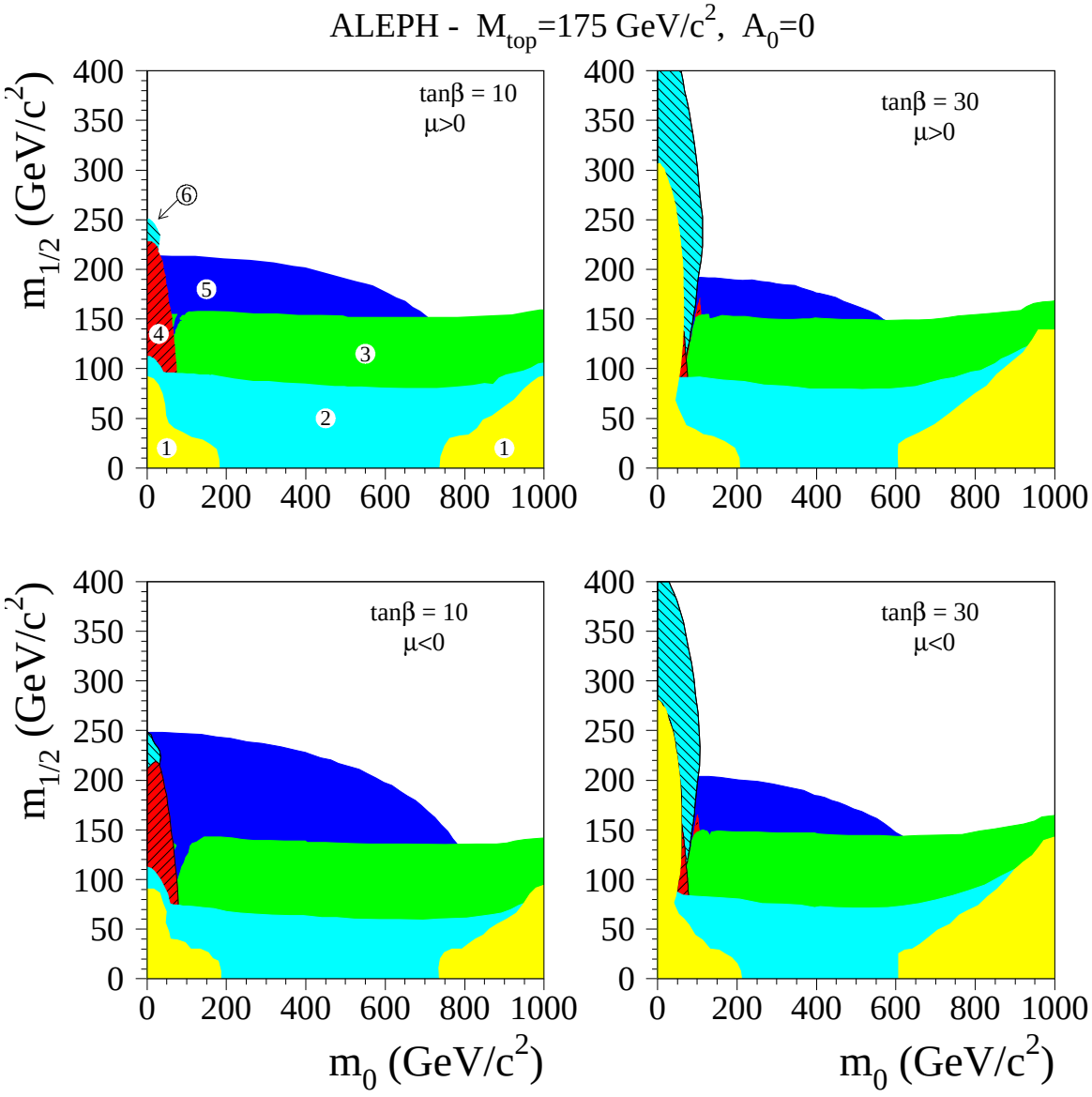

Figure 7: *Minimal Supergravity scenario: domains of the $(m_0, m_{1/2})$ plane excluded for tanβ = 10 and 30 and for $A_0 = 0$. Region 1 is theoretically forbidden. The other regions are excluded by the Z width measurement at LEP1 (2), and by chargino (3), slepton (4), Higgs boson (5) and stable-charged-particle (6) searches at $\sqrt{s} \leq 209$ GeV.*

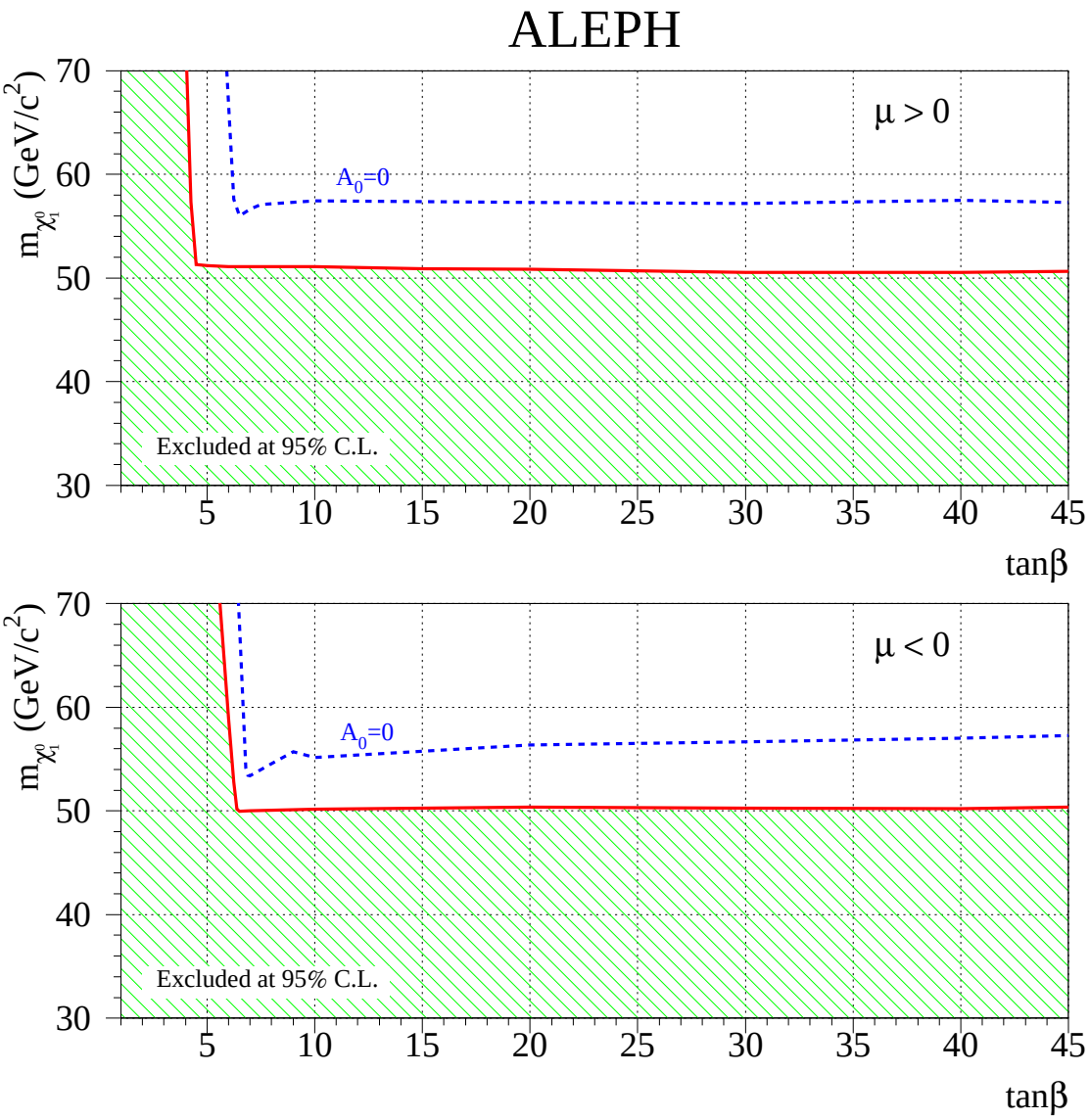

Figure 8: *Minimal Supergravity scenario: lower limit on the LSP mass as a function of tanβ. The dashed line shows the result obtained with $A_0 = 0$. The full line represents the results obtained for the LSP mass limit, independent of the parameter A_0.*